Removal of Some Heavy Metals from Tannery Wastewater Using Activated Carbon from *Neocarya Macrophylla* Seeds

*[a,b]Mohammed, U.M., [b]Jonathan,Y., [c]Abdulkareem, A.S.,
[b]Muhammad, S.A.M., [b]Ndamitso, M.M.
[a]Department of Chemistry, Federal College of Education, Kontagora, Niger State, Nigeria
[b]Department of Chemistry, Federal University of Technology, Minna, Nigeria
[c]Department of Chemical Engineering, Federal University of Technology, Minna, Nigeria
*Correspondence email :mohammedumarmanko@yahoo.com

Abstract

This study presents an analysis of activated carbon derived from Neocarya Macrophylla seeds for the removal of Cr^{3+} and Fe^{3+} ions from tannery wastewater. The activated carbon was prepared using both acid and base. The base-activated carbon exhibited a higher yield compared to the acid-activated carbon. Modification led to an increase in ash content, suggesting chemical interactions' influence on ash content. X-ray diffraction (XRD) analysis revealed miller indices of (002) and (101) for reflection peaks at 28^o and 51.26^o, respectively. Acid modification resulted in sharp and intense peaks, indicating enhanced crystalline size and pore development. High-resolution transmission electron microscopy (HRTEM) and selected area electron diffraction (SAED) confirmed a disordered and porous microstructure, with SAED exhibiting distinct crystalline patterns in base and acid-activated carbon. Fourier-transform infrared (FTIR) spectra indicated various functional groups like OH groups, carbonyl groups, C=C stretching vibrations, C-H stretching vibrations, and Si-O-Si symmetric stretching vibrations in the activated carbon. The study investigated the effects of adsorbent dosage, contact time, and temperature on the adsorption process using batch process techniques. Kinetic and isotherm data were analyzed using the pseudo-first-order and pseudo-second-order models, as well as the Langmuir and Freundlich isotherm models. The findings revealed that the pseudo-second-order and Freundlich models provided the best fit for the data. The results demonstrate that activated carbon is a highly efficient adsorbent for removing heavy metal ions from tannery wastewater.

Keywords: Activated, Adsorbent, Carbon, Isotherm, Kinetic, *Neocarya Macrophylla*

INTRODUCTION

Water pollution presents a significant threat to both human health and the environment, as it involves the discharge of organic and inorganic pollutants into aquatic ecosystems, either in soluble or insoluble forms. This issue is exacerbated by the increasing utilization of substances such as dyes, volatile organic compounds, metals, and disinfectant by-products, primarily due to the rapid pace of industrialization and globalization (Gaur *et al*., 2022). Many of these pollutants are non-biodegradable and highly toxic. For instance, heavy metals originating from wastewater in various industries, including mining, electrical, electroplating, tannery, and smelting, are not only poisonous but also resistant to biological degradation. They pose significant threats to ecosystems and human health as they accumulate in groundwater (Saxena *et al*., 2020). Furthermore, despite being essential for living organisms and critical for enzyme

function in humans, excessive concentrations of these potential toxic elements (PTEs) in the human body can lead to kidney and liver damage, as well as Alzheimer's disease. Therefore, addressing the inadvertent discharge of heavy metals is a pressing environmental concern that must be resolved before contaminated water is reintroduced into the ecosystem.

Numerous methods have been employed to remove heavy metals from industrial wastewater, including electrochemical processes, chemical precipitation, coagulation, membrane filtration, ion exchange, bioremediation, and adsorption. However, many of these treatment techniques have detrimental environmental impacts, limited efficiency, operational constraints, and high costs, which restrict their application (Fouda-Mbanga *et al*., 2021). Among these methods, adsorption stands out as the most effective physicochemical approach for heavy metal removal due to its simplicity, cost-effectiveness, and the regenerative nature of the adsorbents (Abdollahi *et al*., 2022). The adsorbents utilized for heavy metal treatment possess distinctive features like high pore volume and a large surface area, making them valuable for this purpose. Consequently, there has been a growing focus on identifying cost-effective and unconventional sources, such as agricultural and industrial waste, for the production of efficient activated carbons.

The seed of *Neocarya Macrophylla* represents an environment problem as it is hardly biodegradable. *Neocarya Macrophylla* is a tree native to West and Central Africa, belonging to the *Chrysobalancea* family and the *Parinari* genus, with heights ranging from 6 m to 10 m. This study aims to carbonize these seeds to produce active carbons. To date, the efficiency of heavy metal removal from tannery wastewater using acid/base activated carbons in comparison has not been published in the literature. In this study, the efficiency of acid-base activated carbon produced by sequential carbonization and chemical activation techniques was evaluated. The obtained activated carbons were characterized using high-resolution transmission electron microscopy (HRTEM) and X-ray diffraction spectroscopy (XRD). The effect of different factors such as contact time, adsorbent dosage, and temperature on the adsorption of metal ions was investigated. Furthermore, the data obtained under different operating conditions were fitted into different kinetic models and isotherms to determine the kinetics and sorption process.

MATERIALS AND METHODS

Sample Collection and Pre-treatment

The tannery wastewater sample was collected from Majema Tannery industry, Manuri Road, Tudun Wada Area, Sokoto State and placed in a fifty (50) litre container rinsed with diluted *hydrogen trioxonitrate (V)* acid. The wastewater sample was transported to the laboratory for the determination of its physicochemical parameters. *Neocarya macrophylla (NM)* seeds were obtained from farmland; washed under tap water several times followed by deionized water. After thorough washing, they were cut into small pieces and dried under sunlight for weeks to remove all moisture present.

Preparation of Activated Carbon

The dried pieces of *Neocarya macrophylla* seeds were washed with hot water at 70°C to remove any soluble matter present and dried in an oven at 105°C for 48 hours. The oven-dried sample was powdered using a conventional mixer and sieved through a 100µm mesh range. The dried sample was subjected to heating in a furnace for 15 minutes at 550°C and quenched in 0.1 M NaOH/HCl solution. The sample was washed copiously with deionized water until pH 7 was

attained. The sample was then dried in an oven at 105°C for complete dryness. The powdered activated carbon was stored prior to analysis.

Characterization of Activated Carbon

The crystal phases and the crystallite size of the synthesized activated carbon were determined using a Bruker D8 Advance X-ray diffractometer with Cu Kα radiation. The powdered sample was sprinkled on a de-greased glass slide and their diffractograms were recorded. The particle size and distribution pattern were analyzed by Ziess Auriga High-Resolution Transmission Electron Microscopy (HRTEM). About 0.02 g of the synthesized samples was suspended in 10 cm^3 of methanol and thereafter subjected to ultrasonication until complete dispersion was achieved. Two drops of the slurry were dropped onto a holey carbon grid with the aid of a micropipette and subsequently dried by exposure to photolight. Fourier transform infrared spectra (FTIR) of the synthesized samples were recorded using a Perkin-Elmer 2000 FTIR spectrometer fitted with a deuterated triglycine sulphate (DTGS) detector covering the frequency range of 500-4000 cm^{-1}. The sample cell was purged with nitrogen gas throughout data collection to exclude carbon dioxide and water vapour. Ten milligrams (10 mg) of the dried samples were evenly dispersed in 200 mg of spectroscopic grade KBr to record the spectra.

Batch Adsorption Studies

Batch adsorption experiments were conducted to determine the optimum equilibrium time, to generate adsorption kinetics data, and adsorption thermodynamic data. The percent removal and adsorption capacity of heavy metals from digested wastewater solution using activated carbons were calculated by the following equation:

$$\% \text{ Removal} = \frac{C_o - C_f}{C_o} \times 100 \quad (1)$$

$$q_e = \frac{C_o - C_f}{M} V \quad (2)$$

where C_o and C_f are the initial and equilibrium adsorbate concentrations in solution (mg/L), respectively, V is a known volume of synthetic wastewater (L), and M is a known mass of dry adsorbent (g).

The effect of contact time on the metal ions' removal from digested solution using activated carbon was investigated by contacting 0.2 g of the samples with 40 cm^3 of digested wastewater solution and agitated at a speed of 150 rpm for 0, 5, 10, 15, 20, and 25 minutes. The effect of adsorbent dosage on the metal ion removal was investigated by varying the dose at 0.4, 0.6, 0.8, 1.0, and 1.2 g. The impact of temperature was performed at temperatures ranging between 30 to 70°C. The samples were filtered at respective times, and the concentration of metal ions was analyzed using an atomic absorption spectrometer (AAS).

RESULTS AND DISCUSSION

Some Physicochemical Characterization of Activated Carbon

Table 1 presents the percentage yield and bulk density of the activated carbon prepared from *Neocarya Macrophylla* seeds. As can be seen, the base-activated carbon (38.50%) had a significantly higher yield compared to acid-activated carbon (32.03%). The impregnation of acid and base showed an increase in percentage yield and also prevented the release of volatile

matter. This corresponds to the findings of Kosheleva *et al*. (2019), who reported that the chemicals incorporated into the interior of the precursor particles react with the products resulting from the thermal decomposition of the precursor, reducing the evolution of volatile matter and inhibiting the shrinking of the particles; in this way, the conversion of the precursor to carbon is high, and once the chemicals are eliminated after heat treatment, a large amount of porosity is formed.

The moisture content of acid-modified and base-modified carbon is 4.62% and 4.30%, respectively, as presented in Table 1. As seen in Table 1, there is a significant effect of impregnation toward the content of moisture in the sample, suggesting that there would be a correlation between the adsorption capacity of activated carbon and moisture content. The reduction in moisture content leads to better activation of carbon in the adsorption process due to less competition of water vapour within the pores of the sample. Ash is a non-carbon substance that is attached to the surface of the carbon. The values of the ash content increased on the impregnated carbon as represented in Table 1. The base and acid-modified carbon contain 4.2% and 5.8%, respectively. The chemical modification of activated carbon brings about significant changes in the ash content of the produced activated carbon. This could be as a result of interaction of chemicals with the ash content in the activated carbon. The bulk densities of the samples are presented in Table 1. The bulk density of modified activated carbon recorded a low value, and this property can be explained by the low ash contents of the modified activated carbon.

Table 1: Some Characteristics of Activated Carbon

Sample	% Yield	Bulk density (g/cm^3)	Moisture (%)	Ash (%)
Acid-AC	32.03	0.412	4.62	5.8
Base-AC	38.50	0.508	4.30	4.2

Characterization of Activated Carbons

XRD Analysis of Activated Carbon

The phase analysis of modified activated carbon and their XRD patterns are presented in Fig. 1. The diffraction peaks of the samples at 28°, 51.26°, 54.40°, and 68.5° show the amorphous structure of activated carbon due to the reflection of (002), (100), (101), and (010) planes, respectively. The existence of other peaks is attributed to modifiers added to the surface of the carbon. The sharp and intense peaks in the acid-modified sample are due to the enlargement of crystalline size and development of pores. Based on the JCPDS file, the structure of the activated carbon has the Miller indices of (002) and (101) for the reflection peaks at 28° and 51.26°, respectively. Winata *et al*. (2021) observed that two main peaks at 26°, which are attributed to the (002), and 40° correspond to the (101). The XRD patterns also show that samples exhibited uniform pattern changes, with the presence of some peaks associated with the chemical agents in the samples. This might be because of incomplete removal of the chemical agent (binding interaction on the surface) during washing for the neutralization of the yielded activated carbon.

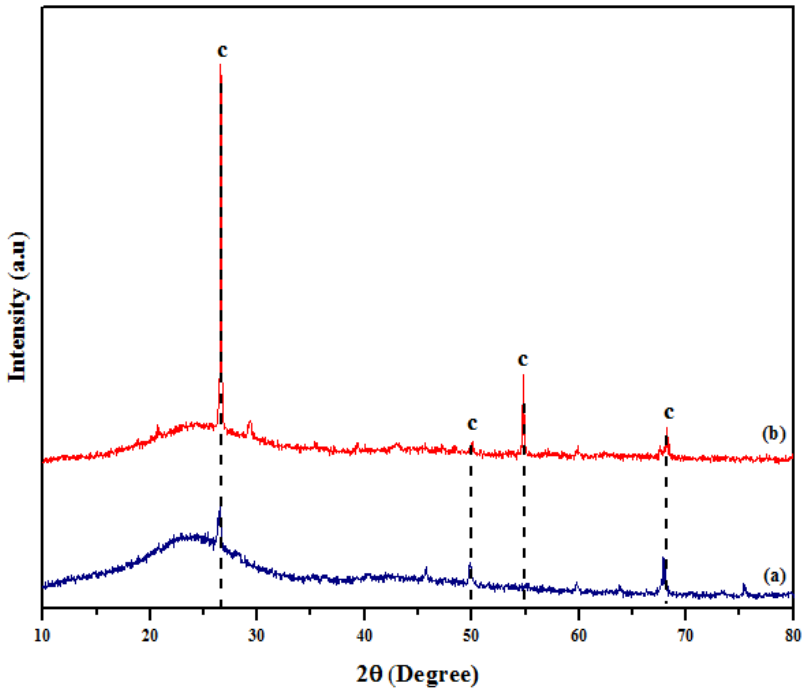

Figure 1: XRD results of (A) acid modified carbon and (B) base modified carbon.

HRTEM and SAED of Activated Carbon

The HRTEM and SAED structures of activated carbon samples are presented in Fig. 2. The carbon materials possess a disordered and porous microstructure consisting of curled carbon layers. The black spots on the images represent the carbon, and the SAED patterns of base and acid activated carbon showed the crystalline and amorphous nature of the materials, respectively. Puspitasari *et al*. (2020) indicated that chitosan hydrogel-based activated carbon nanoparticles were composed of crystallinity and amorphous regions. The SAED rings of the base activated carbon can be indexed to (002) and (101) planes, which correspond to the XRD result.

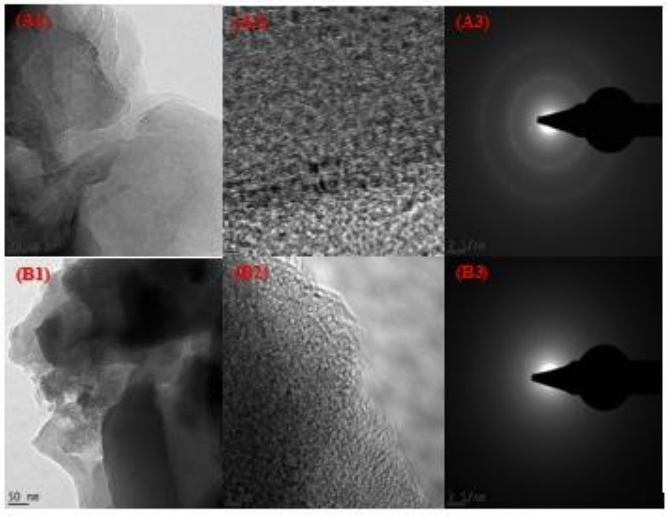

Figure 2: HRTEM results of (A) base modified carbon and (B) acid modified carbon.

FTIR Analysis of Acid and Base Activated Carbon

The FTIR spectra of acid and base activated carbon are shown in Fig. 3. The presence of OH group stretching vibration at the absorption band of 3430 cm^{-1} corresponds to hemicellulose, lignin, and absorbed water molecules. The existence of carbonyl groups is responsible for the absorption band at 1693 cm^{-1}, and the stretching vibrations of C=C at the absorption band of 1590 cm-1 could be attributed to the existence of an aromatic ring in the lignin. The results of the characterization demonstrate that a functional group on a sample surface was relatively near to the findings of Sujiono *et al*. (2022). The presence of C-H stretching vibrations at 2915 and 2850 cm^{-1} might be due to the existence of hemicellulose and cellulose. The presence of the absorption band at 790 cm^{-1} is responsible for the presence of Si-O-Si symmetric stretching vibration.

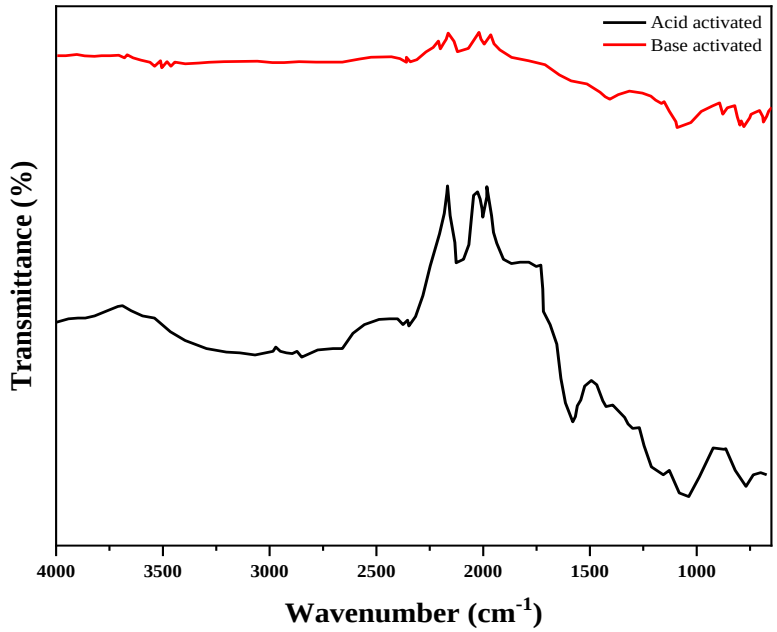

Figure 3: FITR od acid and base-activated carbon.

Batch Adsorption Studies

Effect of Contact Time

The effect of contact time on metal ions removal using acid and base activated carbon was investigated by changing contact time from 0to 25 min (Fig. 4 a and b). The figure shows that the percentage removal of metal ion sorbed increased along with time until equilibrium was reached. At first stage, the metal ion removal was fast due to the large number of active sites existing on the adsorbent which saturated with the passage of time until equilibrium was reached. The high percentage removal achieved using acid activated carbon was 52.23 % for Fe^{3+} and 65.75 % for Cr^{6+} while base activated carbon had 59.82 % for Fe^{3+} and 69.20 % for Cr^{6+}.

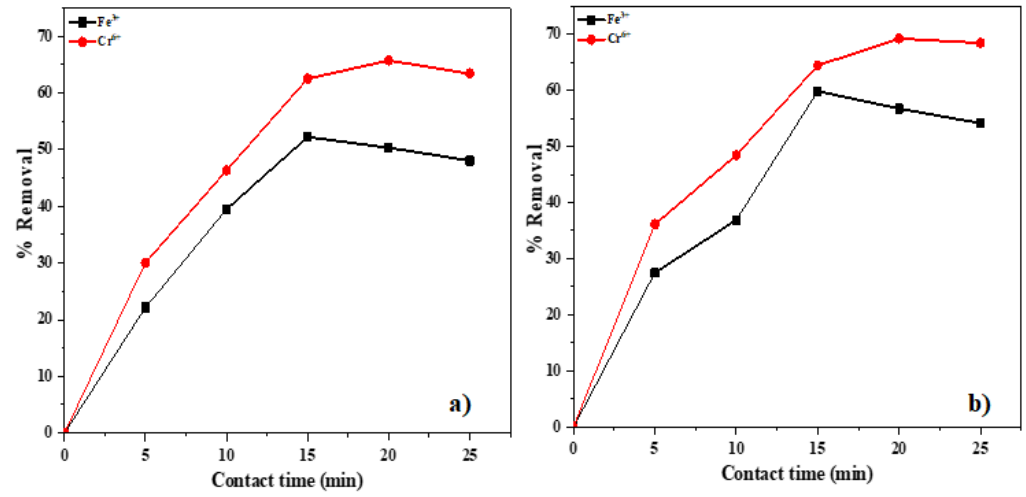

Figure 4: Effect of contact time in the removal of Cr^{+6} and Fe^{3+} from tannery wastewater using (A) acid activated carbon (B) base activated carbon.

Effect of Dosage

The adsorbent dosage showed a significant effect on the removal of metal ions from tannery wastewater as observed by varying the dosage from 0.4 to 1.2 g of acid and base activated carbon (see Fig. 5). The results as presented in Fig. 5(a) indicated that acid activated carbon exhibited percentage removal of 36.64 to 91.23 % for Fe(III) ion and 42.05 to 96.01 % for Cr(VI) ions. The base activated carbon showed the percentage removal of Fe(III) ion from 40.15 to 99.03 % and 51.47 to 100 of Cr(VI) ions removal from tannery wastewater. The migration of heavy metal ions on the adsorbent depends on the ionic/atomic radius of the heavy metals with Cr and Fe ions having ionic radii of 0.052 and 0.0645 nm, respectively. The percentage removal of other heavy metals increases with increasing dosage of the adsorbent'sdosage. This increment may be attributed to the availability of the adsorption sites which is in agreement with the findings of Lui *et al*(2020).

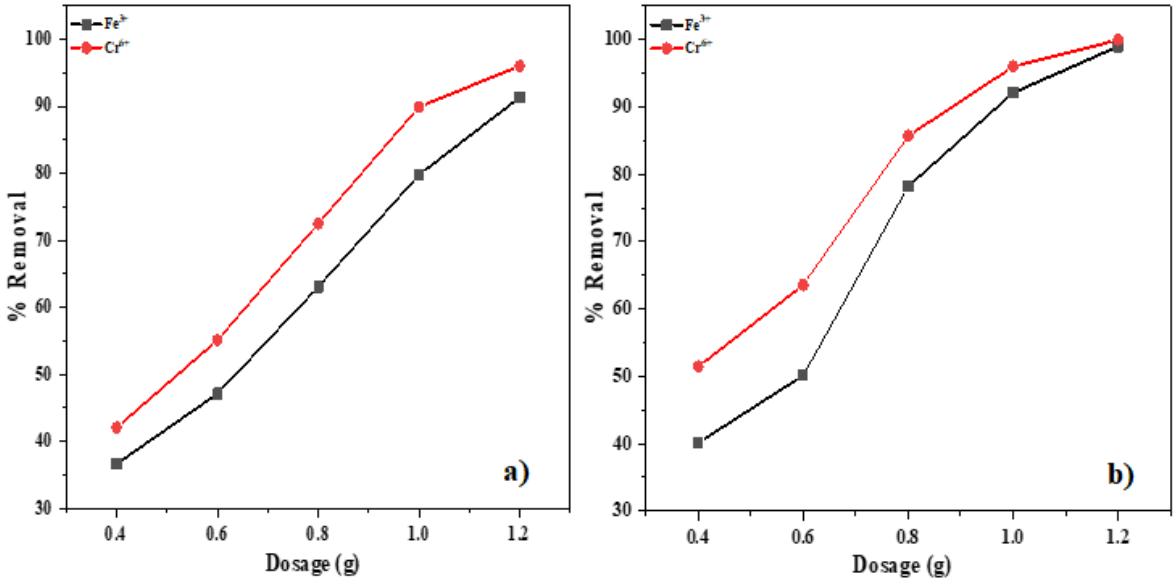

Figure 5: Effect of adsorbent dosage in the removal of Cr^{+6} and Fe^{3+} from tannery wastewater using (A) acid activated carbon (B) base activated carbon.

Effect of Temperature

The removal efficiency Cr(VI) and Fe(III) ions from tannery wastewater with respect to the applied temperature using acid and base activated carbon are shown in Fig. 6. It was noticed that the removal rate of metal ions increases with increasing solution temperature, indicating that the interaction between metal and biosorption is an endothermic process. The variation in the removal of metal ions appears to be linked to the increased tendency of these ions to escape from the aqueous phase into the bulk solution, resulting in a subsequent increase in the thickness of the boundary layer (Masoumi *et al*., 2022). The rise in removal at higher temperatures can also be attributed to the reduced solubility of metals at relatively elevated temperatures.

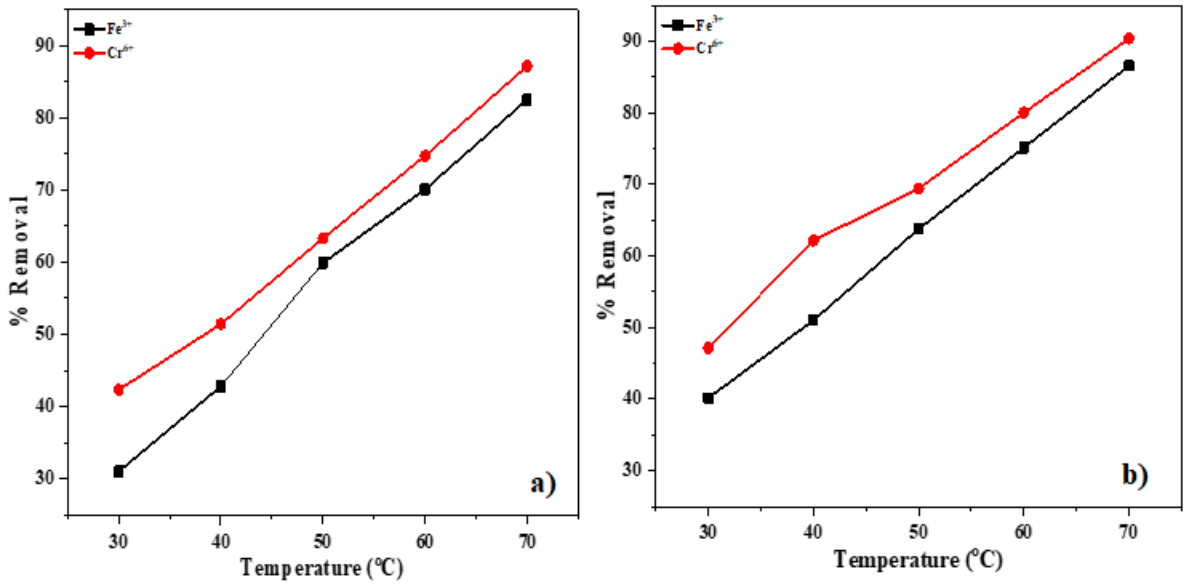

Figure 6: Effect of temperature in the removal of Cr^{+6} and Fe^{3+} from tannery wastewater using (A) acid activated carbon (B) base activated carbon.

Adsorption Isotherm

The linear Langmuir and Freundlich adsorption isotherm equations (3 and 4) are used to calculate the isotherms parameter of the metal ions removal from wastewater as presented in Table 2.

$$\frac{C_e}{q_e} = \frac{1}{bq_m} + \frac{C_e}{q_m} \quad (3)$$

$$\ln q_e = \ln K_f + \frac{1}{n}\ln C_e \quad (4)$$

where C_e is the equilibrium concentration of solution (mg/dm^3), q_e is the adsorption capacity (mg/g), q_m is the maximum adsorption capacity (mg/g) and b is the adsorption equilibrium constant (L/mg), K_f and n are known as Freundlich constants. The sequence of adsorption was determined to be Cr>Fe using acid and base activated carbon. The results from the isotherm study indicate the Langmuir model have higher correlation coefficients (R^2) as displayed in Table 2. This attributes that the adsorbent sites were uniformly distributed across the surface, and metal ions formed mono layers on the sorbent surface. The values of the n_f constant for the Freundlich model were found between 0.2 to 1, suggesting that the adsorption of metal ions on the surface of the adsorbent is favourable.

Table 2: Isotherm Models of Metal ions Removal in Wastewater.

Adsorbent	Metal ion	Langmuir			Freundlich		
		K_L	Q_m	R^2	K_f	n	R^2
Acid activated carbon	Fe	0.0231	40.23	0.9894	2.18	0.226	0.8853
	Cr	0.0261	68.51	0.9936	2.49	0.248	0.9139
Base activated carbon	Fe	0.0613	67.84	0.9971	2.86	0.312	0.9213
	Cr	0.0783	89.71	0.9982	3.14	0.405	0.9404

Adsorption Kinetic Study

The adsorption experimental data were fitted for pseudo-first-order and pseudo-second-order using equ. 5 and 6.

$$\ln(q_e - q_t) = \ln q_e - k_1 t \quad (5)$$

$$\frac{t}{q_t} = \frac{1}{k_2 q_e^2} + \frac{1}{q_e} t \quad (6)$$

where q_e and q_t are the amount of metal ion (mg/g) at equilibrium time and time t, respectively, k_1 is the pseudo-first-order rate constant and k_2 is the pseudo-second-order rate constant. Table 3 shows the kinetic parameters of the adsorbents for the removal of Cr and Fe ions from wastewater. The results indicated that the adsorption process fitted well for pseudo-second-order kinetics for the Cr and Fe ions. The results are also satisfactory to the higher correlation coefficients (R^2) of pseudo-second-order compared to pseudo-first-order model. This indicates that the adsorption mechanism involves chemical sorption interactions between the adsorbent and the metal ions.

Table3: Kinetic Models of Metal ions Removal in Wastewater

Adsorbent	Metal ion	Pseudo-first-order			Pseudo-second-order		
		k_1	q_e	R^2	k_2	q_e	R^2
Acidactivated carbon	Fe	0.0505	26.75	0.8952	0.708	36.66	0.9893
	Cr	0.102	36.72	0.9232	1.382	60.33	0.9910
Base activated carbon	Fe	0.092	45.06	0.9650	1.645	65.74	0.9989
	Cr	0.138	51.09	0.9217	2.936	83.65	0.9992

Thermodynamic Study

The Van't Hoff equations (Equ. 7 to 9) were used to calculate thermodynamic parameters (ΔS°, enthalpy, ΔH°, and the Gibbs free energy, ΔG°) associated with the adsorption of metal ions onto acid and base activated carbon as presented in Table 4. It was observed that the adsorption of metal ions onto the adsorbents is endothermic nature, as indicated by the positive ΔH° values within the adsorption system.

$$K_d = \frac{q_e}{C_e} \quad (7)$$

$$\Delta G = -RT\ln K_d \quad (8)$$

$$\Delta G = \Delta H - T\Delta S \quad (9)$$

where the values of ΔG, ΔH, and ΔS were measured in kJ/mol, kJ/mol, and J/molK respectively. T is the absolute temperature (K), R is the universal gas constant (8.314 J/molK).The ΔS° values were positive for the metal ions, indicating a random adsorption process driven by the increase of energy between the metal ions and the adsorbent. The negative ΔG° values for the

adsorption of metal ions implied that the process occurred spontaneously. Remarkably, the negative ΔG° values increased with rising temperatures, implying favourable increase of spontaneous adsorption process.

Table 4: Thermodynamic Study of Metal ions Removal in Wastewater

Adsorbent	Metal ion			ΔG (kJ/mol)				
		ΔH (kJ /mol)	ΔS (J /molK)	303K	313K	323K	333K	343K
Acid activated carbon	Fe	7.815	28.719	-0.89	-1.17	-1.46	-1.75	-2.04
	Cr	5.626	21.725	-0.96	-1.17	-1.39	-1.61	-1.83
Base activated carbon	Fe	6.092	24.162	-1.23	-1.47	-1.71	-1.95	-2.20
	Cr	7.215	30.284	-1.96	-2.26	-2.57	-2.87	-3.17

CONCLUSION

The study focused on removal of Cr and Fe ions from tannery wastewater using activated carbon from *Neocarya Macrophylla* seeds. The XRD phase analysis of modified activated carbon showed the diffraction peaks of the samples at 28º, 51.26º, 54.40º and 68.5º with the reflection of (002), (100), (101) and (010) planes, respectively. The HRTEM structures of activated carbon samples are porous microstructure consisting of curled carbon layer. The FTIR spectra of acid and base activated carbon indicated the presence of OH group stretching vibration at absorption band of 3430 cm^{-1} related to hemicellulose, lignin, and absorbed water molecules. The batch adsorption processes of the removal of metal ions were influenced by contact time, dosage and temperature. The adsorption isotherm and kinetic data followed Langmuir isotherm and pseudo-second-order model. The thermodynamic parameters confirmed the spontaneous nature of adsorption process. These results show that acid and base activated carbon are potential candidates for the removal of Cr(VI) and Fe(III) ions from tannery wastewater.

References

Abdollahi, N., Moussavi, G., & Giannakis, S. (2022). A review of heavy metals' removal from aqueous matrices by Metal-Organic Frameworks (MOFs): State-of-the art and recent advances. *Journal of Environmental Chemical Engineering*, 10(3), 107394.

Fouda-Mbanga, B. G., Prabakaran, E., & Pillay, K. (2021). Carbohydrate biopolymers, lignin based adsorbents for removal of heavy metals (Cd2+, Pb2+, Zn2+) from wastewater, regeneration and reuse for spent adsorbents including latent fingerprint detection: A review. *Biotechnology Reports*, 30, e00609.

Gaur, N., Dutta, D., Singh, A., Dubey, R., & Kamboj, D. V. (2022). Recent advances in the elimination of persistent organic pollutants by photocatalysis. *Frontiers in Environmental Science*, 10, 872514.

Kosheleva, R. I., Mitropoulos, A. C., &Kyzas, G. Z. (2019). Synthesis of activated carbon from food waste. Environmental Chemistry Letters, 17, 429-438.

Liu, Q., Li, Y., Chen, H., Lu, J., Yu, G., Möslang, M., & Zhou, Y. (2020). Superior adsorption capacity of functionalised straw adsorbent for dyes and heavy-metal ions. *Journal of Hazardous Materials*, 382, 121040.

Masoumi, H., Ghaemi, A., & Gilani, H. G. (2022). Experimental and RSM study of hypercrosslinked polystyrene in elimination of lead, cadmium and nickel ions in single and multi-component systems. *Chemical Engineering Research and Design*, 182, 410-427.

Puspitasari, F. H., Salamah, U., Sari, N. R., Maddu, A., &Solikhin, A. (2020). Potential of chitosan hydrogel based activated carbon nanoparticles and non-activated carbon nanoparticles for water purification. Fibers and Polymers, 21, 701-708.

Saxena, G., Kumar, V., & Shah, M. P. (Eds.). (2020). *Bioremediation for environmental sustainability: toxicity, mechanisms of contaminants degradation, detoxification and challenges*. Elsevier.

Sujiono, E. H., Zabrian, D., Zharvan, V., & Humairah, N. A. (2022). Fabrication and characterization of coconut shell activated carbon using variation chemical activation for wastewater treatment application. Results in Chemistry, 4, 100291.

Winata, A. S., Devianto, H., & Susanti, R. F. (2021). Synthesis of activated carbon from salacca peel with hydrothermal carbonization for supercapacitor application. Materials Today: Proceedings, 44, 3268-3272.